Materials LAB

Perspective

Routes to High-Ranged Thermoelectric Performance

Published as part of the Virtual Special Issue "Mercouri G. Kanatzidis at 65"

Yu Xiao*

State Key Laboratory for Mechanical Behavior of Materials, Xi'an Jiaotong University, Xi'an 710049, China
* Corresponding author, E-mail: xiao_yu@xjtu.edu.cn

Abstract

Thermoelectric technology has immense potential in enabling energy conversion between heat and electricity, and its conversion efficiency is mainly determined by the wide-temperature thermoelectric performance in a given material. Therefore, it is more meaningful to pursue high *ZT* values in a wide temperature range (namely high average *ZT*) rather than the peak *ZT* value at a temperature point. Herein, taking lead chalcogenides as paradigm, some rational routes to high average *ZT* value in thermoelectric materials are introduced, such as bandgap tuning and dynamic doping. This perspective will emphasize the importance of dynamically optimizing carrier and phonon transport properties to high-ranged thermoelectric performance, which could judiciously be extended to other thermoelectric systems.

Key words: thermoelectric material; average *ZT* value; bandgap tuning; dynamic doping

Citation: Yu Xiao. Routes to High-Ranged Thermoelectric Performance. *Materials Lab* 2022, 1, 220025. DOI: 10.54227/mlab.20220025

Main text:

Thermoelectric technology has attracted widespread attentions in energy conversion between heat and electricity because of its characteristics of long service life, high reliability, no noise and pollutant emission *etc*.[1–3] However, its inferior conversion efficiency badly restricts large-scale practical applications. The thermoelectric performance mainly depends on the dimensionless figure of merit, $ZT=\sigma S^2/\kappa T$, where σ, S, κ, T denote electrical conductivity, Seebeck coefficient, thermal conductivity, working temperature in Kelvin, respectively. The thermoelectric conversion efficiency (η) can be evaluated by average *ZT* value (ZT_{ave}) in material as follows:[4,5]

$$\eta = \frac{T_H - T_C}{T_H} \frac{\sqrt{1+ZT_{ave}}-1}{\sqrt{1+ZT_{ave}}+T_C/T_H} \quad (1)$$

$$ZT_{ave} = \frac{\int_{T_C}^{T_H} ZT\,dT}{T_H - T_C} \quad (2)$$

where the T_H and T_C are the temperature at hot side and cold side, and the ZT_{ave} value means the cover area in temperature-dependent *ZT* curve. Obviously, high thermoelectric conversion efficiency demands large ZT_{ave} value and wide working temperature, and it is of great importance to enhance the ZT_{ave} value in thermoelectric material at wide temperature range. However, previous research mainly focused on the enhancement of peak *ZT* value, and many developed strategies only work at a narrow temperature range.[6–8] Commonly used band convergency is always realized at a narrow temperature range and will diverge with increasing temperature.[6] Resonant state can enhance the carrier effective mass but only work at low temperature range.[7,9] Nanostructure is used to reduce thermal conductivity but fails to intensify high-frequency phonon scattering especially at high temperature.[8,10] Although all-scale hierarchical defects are designed to scatter phonon across integrated length scales, they adversely deteriorate the carrier transport and limit the thermoelectric properties at low temperature range.[11,12] Therefore, to achieve high thermoelectric conversion efficiency, it is urgent to develop effective strategies that can fully optimize thermoelectric performance in the whole working temperature range.

This perspective takes lead chalcogenides (Pb*Q*, *Q*=Te, Se and S) as example to introduce some rational strategies for high ZT_{ave} value at wide temperature range. Lead chalcogenide owns cubic crystal structure and high-symmetry electronic band structure. Due to its large off-center vibration of heavy Pb atom and intensified phonon-electron interaction with increasing temperature, the electronic bandgap undergoes a linear increase, from ~ 0.26 eV at 300 K to ~ 0.36 eV at 673 K in PbTe.[13] As the bandgap enlarges in lead chalcogenide, the carrier effective mass (m^*) also continuously rises as a result of band flattening. From single band conduction, the carrier density (n) and carrier effective mass (m^*) should follow intrinsically proportional relation of $n \sim (Tm^*)^{3/2}$ in order to maximize power factor (σS^2).[14,15] Thermoelectric materials with lower carrier effective mass require less carrier, and vice versa, and the optimal carrier density in lead chalcogenide is supposed to dynamically increase with increasing temperature.

In practical terms, the thermoelectric performance in lead chalcogenide is commonly tuned by heavily static doping with donor or acceptor dopant. In static doping sample (*n*-type lead chalcogenide), the carrier density always maintains at a constant with increasing temperature. The optimal relation of $n \sim (Tm^*)^{3/2}$ between carrier density and carrier effective mass can only be obtained at narrow temperature range,

Received 12 April 2022; Accepted 20 April 2022; Published online

which can lead to a peak *ZT* value but limit the thermoelectric performance at low temperature. To optimize its thermoelectric performance in the whole working temperature range, the bandgap is firstly narrowed to facilitate electrical transport properties near room temperature. It is proved that Sn alloying in lead chalcogenide can cause a band sharpening at low Sn content, and large Sn alloying content will cause band inversion between conduction band and valence band.[16,17] In the process of band sharpening, the carrier effective mass in Sn-alloyed lead chalcogenide will continuously decrease, which can benefit high carrier mobility. Furthermore, heavily Sn alloying in lead chalcogenide will import massive point defects and favorably intensify phonon scattering to reduce lattice thermal conductivity. Although these Sn atomic defects will also cause carrier scattering, the reduced carrier effective mass in Sn-alloyed lead chalcogenide will compensate the carrier mobility, and finally maintains high electrical transport properties.

After bandgap tuning in lead chalcogenide, the carrier density should be re-optimized and dynamic doping is necessary to make the carrier density well match its temperature-dependent carrier effective mass. This dynamically optimized relation between n and m^* can further contribute to high temperature-dependent carrier mobility and power factor in the whole working temperature range. From previous results, dynamic doping can be achieved by importing small-size atoms (such as Cu[18,19], Ag[20] or Zn[21]) into interstitial sites in cubic lead chalcogenide, which can work as donor dopant and provide extra electron in *n*-type lead chalcogenide. When temperature increases, the solubility of these small-size atoms in lead chalcogenide rises owning to lattice expansion, thus causing an increasing temperature-dependent carrier density in *n*-type lead chalcogenide. Besides small-size interstitial doping, mixed valence states elements (such as Ga[22] and In[23,24]) can also be used to realize dynamic carrier density manipulation in *n*-type lead chalcogenide. These amphoteric Ga/In elements present mixed valence states (+1 and +3) and can form defect level in matrix to work as electron reservoir. With temperature increasing, low valence state (+1) will be thermally activated into high valence state (+3), and simultaneously release two free electrons from defect level into conduction band, thus dynamically optimize the carrier density. Notably, the dynamic doping behavior is only found in *n*-type lead chalcogenide, therefore it is important to explore new methods to realize similar dynamic doping in *p*-type lead chalcogenide.

With these successive strategies above, from static doping, bandgap tuning to dynamic doping (Figure 1a), the temperature-dependent *ZT* value in lead chalcogenide is firstly amplified near room temperature and then largely enhanced in the whole working temperature range (Figure 1b). This case in lead chalcogenide clarifies the impacts of dynamic optimization between carrier effective mass and carrier density on enhancing ZT_{ave} value. In fact, the aim of synergistically manipulating carrier effective mass and carrier density is to maintain high carrier mobility in thermoelectric materials, because high carrier mobility is crucial to achieve large ZT_{ave} value.[25] It is worth noting that band alignment is another effective strategy to maintain high carrier mobility. When exotic phase is introduced to reduce lattice thermal conductivity in thermoelectric materials, the carrier mobility will inevitably be impaired due to stain filed and energy barrier at phase interface. To maintain high carrier mobility, the electronic band structure can be tuned to well align in energy and weaken the energy scattering to carrier. Results have proved that the strategy of band alignment can be applied in both *n*-type and *p*-type lead chalcogenide, such as *p*-type PbTe-SrTe,[12,26] *p*-type PbS-CdS,[27] *n*-type PbS-PbTe[28] *etc*.

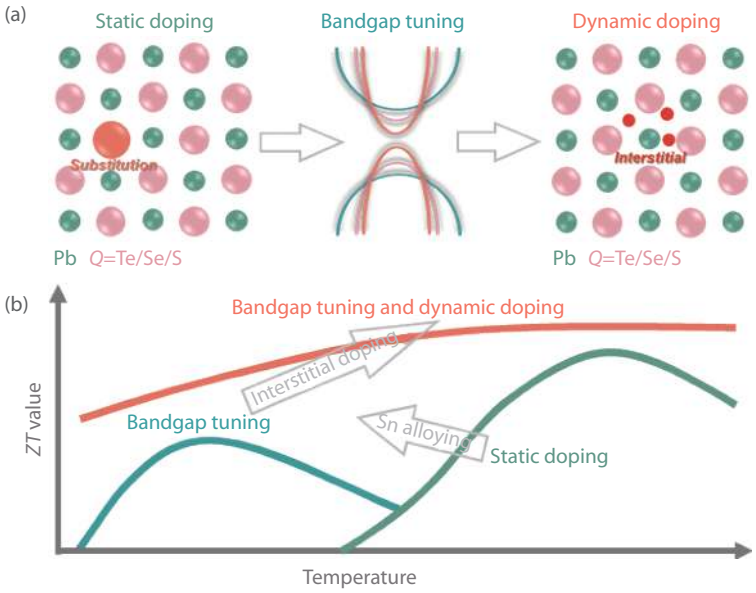

Fig. 1 (a) Strategies to optimize thermoelectric performance, including static doping, bandgap tuning, and dynamic doping. (b) Routes to high average *ZT* value.

Recently, some newly discovered materials featured with large bandgap, low-symmetry and layered crystal structure presented promising thermoelectric performance, such as SnSe,[29–33] SnS[34–36] and $Sb_2Si_4Te_6$.[37] High ZT_{ave} values of ~ 1.9 and ~ 1.7 have been reported in *p*-type SnSe[38] and *n*-type SnSe,[39] respectively. These high thermoelectric properties in SnSe originate from dynamically optimized carrier and phonon transport through multi-band synglisis[35,38] and continu-

DOI: 10.54227/mlab.20220025

ous phase transition.[30,39] These results highlight the importance of dynamically optimizing carrier and phonon transport properties to obtain high ZT_{ave} value, and also intrigue great interest for high ZT_{ave} value in other thermoelectric materials.

Acknowledgments

The author acknowledges the Fundamental Research Funds for the Central Universities (xtr042021007), National Natural Science Foundation of China (52172236), the financial support from the Top Young Talents Programme of Xi'an Jiaotong University.

Conflict of interest

The author declares no conflict of interest.

REFERENCES

1. F. Zhang, D. Wu and J. He, *Materials Lab*, 2022, 1, 220012
2. Y.-T. Fan and G.-J. Tan, *Materials Lab*, 2022, 1, 220008
3. N. Dragoe, *Materials Lab*, 2022, 1, 220001
4. W. Liu and S. Bai, *J. Materiomics*, 2019, 5, 321
5. X. Zhang and L.-D. Zhao, *J. Materiomics*, 2015, 1, 92
6. Y. Pei, X. Shi, A. LaLonde, H. Wang, L. Chen and G. J. Snyder, *Nature*, 2011, 473, 66
7. J. P. Heremans, V. Jovovic, E. S. Toberer, A. Saramat, K. Kurosaki, A. Charoenphakdee, S. Yamanaka and G. J. Snyder, *Science*, 2008, 321, 554
8. B. Poudel, Q. Hao, Y. Ma, Y. Lan, A. Minnich, B. Yu, X. Yan, D. Wang, A. Muto and D. Vashaee, *Science*, 2008, 320, 634
9. Q. Zhang, H. Wang, W. Liu, H. Wang, B. Yu, Q. Zhang, Z. Tian, G. Ni, S. Lee, K. Esfarjani, G. Chen and Z. Ren, *Energy Environ. Sci.*, 2012, 5, 5246
10. K. F. Hsu, S. Loo, F. Guo, W. Chen, J. S. Dyck, C. Uher, H. Tim, E. K. Polychroniadis and M. G. Kanatzidis, *Science*, 2004, 303, 818
11. K. Biswas, J. He, I. D. Blum, C.-I. Wu, T. P. Hogan, D. N. Seidman, V. P. Dravid and M. G. Kanatzidis, *Nature*, 2012, 489, 414
12. G. Tan, F. Shi, S. Hao, L.-D. Zhao, H. Chi, X. Zhang, C. Uher, C. Wolverton, V. P. Dravid and M. G. Kanatzidis, *Nat. Commun.*, 2016, 7, 12167
13. Y. Xiao, H. Wu, J. Cui, D. Wang, L. Fu, Y. Zhang, Y. Chen, J. He, S. J. Pennycook and L.-D. Zhao, *Energy Environ. Sci.*, 2018, 11, 2486
14. C. Fu, S. Bai, Y. Liu, Y. Tang, L. Chen, X. Zhao and T. Zhu, *Nat. Commun.*, 2015, 6, 8144
15. Y. Pei, Z. M. Gibbs, A. Gloskovskii, B. Balke, W. G. Zeier and G. J. Snyder, *Adv. Energy Mater.*, 2014, 4, 1400486
16. S.-Y. Xu, C. Liu, N. Alidoust, M. Neupane, D. Qian, I. Belopolski, J. D. Denlinger, Y. J. Wang, H. Lin, L. A. Wray, G. Landolt, B. Slomski, J. H. Dil, A. Marcinkova, E. Morosan, Q. Gibson, R. Sankar, F. C. Chou, R. J. Cava, A. Bansil and M. Z. Hasan, *Nat. Commun.*, 2012, 3, 1192
17. P. Dziawa, B. J. Kowalski, K. Dybko, R. Buczko, A. Szczerbakow, M. Szot, E. Łusakowska, T. Balasubramanian, B. M. Wojek, M. H. Berntsen, O. Tjernberg and T. Story, *Nat. Mater.*, 2012, 11, 1023
18. L. You, Y. Liu, X. Li, P. Nan, B. Ge, Y. Jiang, P. Luo, S. Pan, Y. Pei, W. Zhang, G. J. Snyder, J. Yang, J. Zhang and J. Luo, *Energy Environ. Sci.*, 2018, 11, 1848
19. L. You, J. Zhang, S. Pan, Y. Jiang, K. Wang, J. Yang, Y. Pei, Q. Zhu, M. T. Agne, G. J. Snyder, Z. Ren, W. Zhang and J. Luo, *Energy Environ. Sci.*, 2019, 12, 3089
20. Y. Pei, A. F. May and G. J. Snyder, *Adv. Energy Mater.*, 2011, 1, 291
21. X. Qian, D. Wang, Y. Zhang, H. Wu, S. J. Pennycook, L. Zheng, P. F. P. Poudeu and L.-D. Zhao, *J. Mater. Chem. A*, 2020, 8, 5699
22. X. Su, S. Hao, T. P. Bailey, S. Wang, I. Hadar, G. Tan, T. B. Song, Q. Zhang, C. Uher and C. Wolverton, *Adv. Energy Mater.*, 2018, 8, 1800659
23. Q. Zhang, Q. Song, X. Wang, J. Sun, Q. Zhu, K. Dahal, X. Lin, F. Cao, J. Zhou and S. Chen, *Energy Environ. Sci.*, 2018, 11, 933
24. Y. Xiao, H. Wu, D. Wang, C. Niu, Y. Pei, Y. Zhang, I. Spanopoulos, I. T. Witting, X. Li, S. J. Pennycook, G. J. Snyder, M. G. Kanatzidis and L.-D. Zhao, *Adv. Energy Mater.*, 2019, 9, 1900414
25. B. Qin and L.-D. Zhao, *Materials Lab*, 2022, 1, 220004
26. K. Biswas, J. He, Q. Zhang, G. Wang, C. Uher, V. P. Dravid and M. G. Kanatzidis, *Nat. Chem.*, 2011, 3, 160
27. L.-D. Zhao, J. He, S. Hao, C. I. Wu, T. P. Hogan, C. Wolverton, V. P. Dravid and M. G. Kanatzidis, *J. Am. Chem. Soc.*, 2012, 134, 16327
28. Y. Xiao, D. Wang, Y. Zhang, C. Chen, S. Zhang, K. Wang, G. Wang, S. J. Pennycook, G. J. Snyder, H. Wu and L.-D. Zhao, *J. Am. Chem. Soc.*, 2020, 142, 4051
29. L.-D. Zhao, S. H. Lo, Y. Zhang, H. Sun, G. Tan, C. Uher, C. Wolverton, V. P. Dravid and M. G. Kanatzidis, *Nature*, 2014, 508, 373
30. C. Chang, M. Wu, D. He, Y. Pei, C.-F. Wu, X. Wu, H. Yu, F. Zhu, K. Wang, Y. Chen, L. Huang, J.-F. Li, J. He and L.-D. Zhao, *Science*, 2018, 360, 778
31. Y. Xiao and L.-D. Zhao, *Science*, 2020, 367, 1196
32. L.-D. Zhao, G. Tan, S. Hao, J. He, Y. Pei, H. Chi, H. Wang, S. Gong, H. Xu, V. P. Dravid, C. Uher, G. J. Snyder, C. Wolverton and M. G. Kanatzidis, *Science*, 2016, 351, 141
33. D. Liu, B. Qin and L.-D. Zhao, *Materials Lab*, 2022, 1, 220006
34. W. He, D. Wang, J.-F. Dong, Y. Qiu, L. Fu, Y. Feng, Y. Hao, G. Wang, J. Wang, C. Liu, J.-F. Li, J. He and L.-D. Zhao, *J. Mater. Chem. A*, 2018, 6, 10048
35. W. He, D. Wang, H. Wu, Y. Xiao, Y. Zhang, D. He, Y. Feng, Y.-J. Hao, J.-F. Dong, R. Chetty, L. Hao, D. Chen, J. Qin, Q. Yang, X. Li, J.-M. Song, Y. Zhu, W. Xu, C. Niu, X. Li, G. Wang, C. Liu, M. Ohta, S. J. Pennycook, J. He, J.-F. Li and L.-D. Zhao, *Science*, 2019, 365, 1418
36. H. Wu, X. Lu, G. Wang, K. Peng, H. Chi, B. Zhang, Y. Chen, C. Li, Y. Yan, L. Guo, C. Uher, X. Zhou and X. Han, *Adv. Energy Mater.*, 2018, 8, 1800087
37. Y. Luo, S. Cai, S. Hao, F. Pielnhofer, I. Hadar, Z.-Z. Luo, J. Xu, C. Wolverton, V. P. Dravid and A. Pfitzner, *Joule*, 2020, 4, 159
38. B. Qin, D. Wang, X. Liu, Y. Qin, J.-F. Dong, J. Luo, J.-W. Li, W. Liu, G. Tan, X. Tang, J.-F. Li, J. He and L.-D. Zhao, *Science*, 2021, 373, 556
39. L. Su, D. Wang, S. Wang, B. Qin, Y. Wang, Y. Qin, Y. Jin, C. Chang and L.-D. Zhao, *Science*, 2022, 375, 1385

Biography

Yu Xiao is an associate professor of the School of Materials Science and Engineering at Xi'an Jiaotong University, China. He received Ph.D. degree from Beihang University, China, in 2019. He was a postdoctoral fellow at Beihang University from 2019 to 2021. His research mainly focuses on band structure and microstructure in thermoelectric materials.